# Geometric bounds on the power of adiabatic thermal machines

Joshua Eglinton◉ and Kay Brandner◉

*School of Physics and Astronomy, University of Nottingham, Nottingham NG7 2RD, United Kingdom*
*and Centre for the Mathematics and Theoretical Physics of Quantum Non-equilibrium Systems,*
*University of Nottingham, Nottingham NG7 2RD, United Kingdom*

We analyze the performance of slowly driven meso- and microscale refrigerators and heat engines that operate between two thermal baths with a small temperature difference. Using a general scaling argument, we show that such devices can work arbitrarily close to their Carnot limit only if heat leaks between the baths are fully suppressed. Their power output is then subject to a universal geometric bound that decays quadratically to zero at the Carnot limit. This bound can be asymptotically saturated in the quasistatic limit if the driving protocols are suitably optimized and the temperature difference between the baths goes to zero with the driving frequency. These results hold under generic conditions for any thermodynamically consistent dynamics admitting a well-defined adiabatic-response regime and a generalized Onsager symmetry. For illustration, we work out models of a qubit-refrigerator and a coherent charge pump operating as a cooling device.

*Introduction.* Dimensionless figures of merit, such as the efficiency of a heat engine or the coefficient of performance (COP) of a refrigerator, provide convenient measures for the performance of thermal machines. These figures are subject to universal bounds, which follow directly from the first and the second law of thermodynamics and are known as Carnot bounds [1]. To attain its Carnot bound, a thermal machine has to work without producing any net entropy. This condition is generally assumed to be met only if the machine does not exchange any heat with its environment or if it operates infinitely slowly. In both cases the generated output per time is zero. Hence, the Carnot limit can be reached only at the price of vanishing power.

The questions of (i) how the tradeoff between power and efficiency can be formulated quantitatively for meso- and microscale thermal machines, and (ii) whether it can be overcome in special situations, have attracted significant interest over the past decade [2–12]. As a result, a variety of tradeoff relations that bound the power of different types of machines in terms of a dimensionless figure of merit were discovered, first in linear-response [13–18] and then far from equilibrium [19–29]. Since such bounds must go beyond the first and the second law, which due to the lack of a fundamental timescale do not provide any constraint on power, they have to be derived from the underlying dynamics of the system. As a result, different bounds hold for Markov jump processes [19–22], underdamped Fokker-Planck dynamics [19], Lindblad dynamics [23,25] or coherent transport [26–28].

For adiabatic thermal machines, which use a working system that is driven by slow periodic variations of external control parameters, thermodynamic geometry provides a promising avenue towards a unified picture. This framework was originally developed for macroscopic systems [30–33] and later extended to classical meso- and microscale systems [34–37] as well as the quantum regime [38–40]. The key idea

is that the time-dependent state variables of the working system, e.g., the entries of a density matrix, which in general have to be found by solving a nonautonomous set of differential equations, become functions of the control variables and their time derivatives if the driving is slow on some characteristic timescale of the system. Quantities such as work or entropy production, which depend on these state variables, can thus be related to geometric objects such as vector fields or metrics in the space of control parameters. Once the dynamics of the system has been specified, the coefficients defining these objects can be calculated by means of adiabatic perturbation theory [41–43]. Any relation between the quantities of interest, however, that follows from general symmetries or purely geometric arguments, holds universally for any kind of thermodynamically consistent dynamics.

The geometric approach has led to notable insights on the principles that govern the performance of adiabatic thermal machines [44–55]. Recent results include explicit optimization schemes for different types of devices [56–63] as well as geometric tradeoff relations between the efficiency, power yield [46] and power fluctuations [51] of cyclic heat engines that are driven by continuous temperature variations. These tradeoff relations show that, close to the Carnot limit, the power of such devices is bounded by a linear function of their efficiency, which goes to zero at the Carnot value.

In this article, we consider a complementary setting, where an adiabatic machine works between two thermal baths with fixed temperatures. The thermodynamic geometry of this setup, which covers both heat engines and refrigerators, is usually developed by treating the temperature difference between the reservoir and the environment as a first-order perturbation along with the driving rates [56]. Here, we argue that this approach is no longer sufficient if the machine operates close to the Carnot limit. Specifically, we show that, in this regime, the performance of a generic machine is governed

by second-order corrections in the temperature difference between the baths. This effect leads to a new family of geometric tradeoff relations implying a quadratic rather than a linear decay of power at the Carnot bound.

*Universal bound on power.* This behavior can be derived from a general scaling argument. To this end, it is convenient to introduce generalized fluxes $J_x$ and affinities $A_x$ such that the average rate of entropy production can be expressed in the standard form $\sigma = J_x A_x$, where summation over identical indices is understood throughout [64]. The fluxes $J_x$ correspond to output and input of the machine, and the affinities $A_x$ represent the thermodynamic forces that drive the system away from equilibrium. For an adiabatic-response theory, natural choices of these variables are [28,42,56]

$$J_w = W, \quad J_q = Q/\tau, \quad A_w = \beta_e/\tau, \quad \text{and} \quad A_q = \beta_e - \beta_r. \tag{1}$$

Here, $\tau$ denotes the cycle time; $\beta_e$ and $\beta_r$ are the inverse temperatures of the two baths, to which we refer as environment and reservoir; and $W$ and $Q$ are the applied work and the heat uptake from the reservoir per operation cycle. Boltzmann's constant is set to 1 throughout. From here on we use $J_w$ and $W$ interchangeably.

We now focus on refrigerators. That is, we assume that $\beta_r \geqslant \beta_e$ and $W, Q \geqslant 0$ so that the machine absorbs work from the external driving and extracts heat from the cold reservoir. The performance of such a device is described by the COP $\varepsilon \equiv Q/W$, which is bounded by the Carnot value $\varepsilon_C \equiv \beta_e/(\beta_r - \beta_e)$. To determine under what conditions $\varepsilon$ approaches $\varepsilon_C$, we divide the work input into an isothermal part and a correction stemming from the temperature difference between the reservoirs,

$$J_w^{\text{iso}} \equiv J_w|_{A_q=0} \equiv K_{ww}A_w \quad \text{and} \quad J_w - J_w^{\text{iso}} \equiv K_{wq}A_q. \tag{2}$$

Analogously, the heat flux can be divided into a quasistatic contribution and a finite-rate correction,

$$J_q^{\text{qs}} \equiv J_q|_{A_w=0} \equiv K_{qq}A_q \quad \text{and} \quad J_q - J_q^{\text{qs}} \equiv K_{qw}A_w. \tag{3}$$

The coefficients $K_{xy}$ are functions of the affinities, which in general assume finite values in the limit $A_x \to 0$. Furthermore, the second law requires that $K_{ww}, K_{qq} \geqslant 0$, and time-reversal symmetry implies that the cross-coefficients obey the Onsager symmetry

$$K_{qw}|_{A_x=0} = -K_{wq}|_{A_x=0} \tag{4}$$

in zeroth order with respect to the affinities. This symmetry holds for arbitrary driving protocols as long as the system is not subject to external magnetic fields breaking time reversal symmetry, which we assume here.

The normalized COP can now be written in the form

$$\frac{\varepsilon}{\varepsilon_C} = -\frac{J_q A_q}{J_w A_w} = -\frac{K_{qw} + K_{qq}(A_q/A_w)}{K_{wq} + K_{ww}(A_w/A_q)}. \tag{5}$$

Since the isothermal work in general will not vanish, it is natural to assume that $K_{ww} > 0$. Due to the Onsager symmetry (4), the expression (5) then converges to 1 in the quasistatic limit $A_w \to 0$ if $K_{qq} = 0$ and $A_q \propto A_w^\alpha$ with $0 < \alpha < 1$. Close to this limit, we can generally assume that $\tau$ is much larger than the typical relaxation time of the system. Provided that

the quasistatic heat flux, $J_q^{\text{qs}}$, vanishes, the Carnot bound is attained asymptotically as both affinities go to zero with $A_w$ vanishing faster than $A_q$, whereby both $\varepsilon$ and $\varepsilon_C$ diverge. The quasistatic heat flux corresponds to the heat exchanged between reservoir and environment in a quasistatic cycle divided by the period. We refer to this quantity as *heat leak*. Provided the quasistatically exchanged heat does not scale with the period, the heat leak vanishes. As we discuss further on, this situation can be realized for instance by decoupling the working system from either the reservoir or the environment at every point of the cycle [4,45,65]. To determine how the cooling power $J_q$ decays in this limit, we expand the coefficients $K_{qw}$ and $K_{wq}$ in the affinities, keeping leading and first subleading terms, $K_{qw} = L_{qw} + L_{qw}^q A_q$ and $K_{wq} = -L_{qw} + L_{wq}^q A_q$. Note that, since $A_w$ is assumed to be of higher order than $A_q$, no contributions proportional to $A_w$ appear in these expansions. Thus, upon keeping only terms that remain significantly close to the quasistatic limit, the generalized fluxes become

$$J_w = L_{ww}A_w + L_{wq}A_q + L_{wq}^q A_q^2, \tag{6a}$$

$$J_q = L_{qw}A_w + L_{qw}^q A_w A_q. \tag{6b}$$

Inserting these expansions into Eq. (5) and again keeping only leading and first subleading terms leaves us with

$$\frac{\varepsilon}{\varepsilon_C} = 1 + \frac{L_{qw}^q + L_{wq}^q}{L_{qw}}A_q + \frac{L_{ww}}{L_{qw}}\frac{A_w}{A_q}, \tag{7}$$

where $L_{ww} \equiv K_{ww}|_{A_x=0}$. Upon maximizing the right-hand side of this equation with respect to $A_q$, we obtain an upper bound on $\varepsilon/\varepsilon_C$ and an optimum for the thermal gradient, which are given by

$$\varepsilon/\varepsilon_C \leqslant 1 - \sqrt{L_{qw}A_w/Z} \quad \text{and} \quad A_q^* = -\sqrt{zA_w} \tag{8}$$

with $Z \equiv L_{qw}^3/4(L_{wq}^q + L_{qw}^q)L_{ww}$ and $z \equiv L_{ww}/(L_{wq}^q + L_{qw}^q)$ being non-negative quantities [66]. The bound (8) is saturated only if the difference in inverse temperature between the environment and reservoir are chosen such that $A_q = A_q^*$. Thus, $A_q$ has to vanish as the driving period becomes infinite, $A_w \to 0$. This result holds for any device where $A_q$ and $A_w$ can be controlled independently. Since $J_q = L_{qw}A_w$ in leading order, we can now replace $A_w$ with $J_q/L_{qw}$ in Eq. (8), which yields the power-COP tradeoff relation

$$J_q \leqslant Z(\varepsilon_C - \varepsilon)^2/\varepsilon_C^2. \tag{9}$$

This relation, which is our first main result, shows that the cooling power of a generic adiabatic refrigerator decays at least quadratically at the Carnot bound.

A similar picture emerges for adiabatic heat engines, which are realized for $\beta_r \leqslant \beta_e$, $Q \geqslant 0$, and $W \leqslant 0$. Hence, the machine picks up heat from the hot reservoir and generates work output. Its efficiency is then defined as $\eta \equiv -W/Q$ and the corresponding Carnot bound reads $\eta_C \equiv (\beta_e - \beta_r)/\beta_e$. Upon introducing the normalized efficiency $\eta/\eta_C = -J_w A_w/J_q A_q$, the steps that lead to Eq. (9) can be repeated one by one [67]. We thus find that $\eta/\eta_C$ generically converges to 1 only if the quasistatic heat flux vanishes and both affinities go to zero with $A_w$ vanishing faster than $A_q$, whereby $\eta$ and $\eta_C$ both approach zero. Close to this limit, the engine is subject to the

power-efficiency tradeoff relation

$$P \leqslant Z(\eta_C - \eta)^2/\eta_C, \tag{10}$$

and the optimal thermal gradient, for which it is saturated asymptotically, is given by $A_q^* = \sqrt{zA_w}$.

The bounds (9) and (10) ultimately arise from the fact that the Onsager symmetry (4) does not extend to the second-order coefficients $L_{wq}^q$ and $L_{qw}^q$. Still, there are special situations, where $L_{wq}^q \simeq -L_{qw}^q$ [67]. Under this condition, the second term in the expansion (7) can be neglected and we are left with the trivial relation $\varepsilon = (1 + L_{ww}A_w/L_{qw}A_q)\varepsilon_C$ [68]. The Carnot bound is then attained for any $A_q$ in the limit $A_w \to 0$ with the power of the machine vanishing linearly. However, this behavior will typically occur only in fine-tuned systems. We stress that this restriction appears only when subleading terms in the expansions of the generalized fluxes are taken into account; cf. Eq. (6). It is therefore not captured by the established adiabatic-response theory, where both fluxes are assumed to be linear in affinities [56].

*Geometric picture.* To unveil the geometric character of the bounds (9) and (10), we have to analyze the structure of $Z$. We assume that the machine is driven by periodic changes of the parameters $\boldsymbol{\lambda} = \{\lambda^\mu\}$, which control the energy of the working system and its coupling to the baths. Once the system has settled to a periodic state, the work input and heat uptake from the reservoir per cycle are given by

$$W = -\int_0^\tau dt\, f_t^\mu \dot{\lambda}_t^\mu \quad \text{and} \quad Q = \int_0^\tau dt\, j_t \tag{11}$$

where $f_t^\mu$ is the generalized force conjugate to the parameter $\lambda^\mu$ and $j_t$ denotes the heat current from the reservoir into the system. If the driving is slow on the internal timescale of the system, and the difference between the inverse temperatures of the reservoir and the environment is small on its typical energy scale, then these quantities can be expanded in the driving rates and the thermal gradient,

$$f_t^\mu = -\partial_\mu \mathcal{F}_{\lambda_t} - \mathcal{R}_{\lambda_t}^{\mu\nu} \beta_e \dot{\lambda}_t^\nu - \mathcal{R}_{\lambda_t}^{\mu q} A_q - \mathcal{R}_{\lambda_t}^{\mu qq} A_q^2, \tag{12a}$$

$$j_t = \mathcal{R}_{\lambda_t}^{q\mu} \beta_e \dot{\lambda}_t^\mu + \mathcal{R}_{\lambda_t}^{qq\mu} \beta_e \dot{\lambda}_t^\mu A_q. \tag{12b}$$

The free energy of the system $\mathcal{F}_\lambda$ and the adiabatic-response coefficients $\mathcal{R}_\lambda$ depend parametrically on the control vector $\boldsymbol{\lambda}$ and on $\beta_e$. Note that we include only the relevant second-order terms and assume that there are no heat leaks, i.e., $j_t|_{\dot{\lambda}_t=0} = 0$.

Upon inserting Eqs. (12) into Eq. (11) and comparing the result with the expansions of the fluxes (6), the off-diagonal coefficients can be expressed as line integrals in the space of control parameters,

$$\begin{bmatrix} L_{wq} & L_{qw} \\ L_{wq}^q & L_{qw}^q \end{bmatrix} = \oint_\gamma \begin{bmatrix} \mathcal{A}_\lambda^{\mu q} & \mathcal{A}_\lambda^{q\mu} \\ \mathcal{A}_\lambda^{\mu qq} & \mathcal{A}_\lambda^{qq\mu} \end{bmatrix} d\lambda^\mu. \tag{13}$$

Here, $\gamma$ denotes the closed path that is mapped out by the driving protocols $\boldsymbol{\lambda}_t$, and the thermodynamic vector potentials are defined as

$$\begin{bmatrix} \mathcal{A}_\lambda^{\mu q} & \mathcal{A}_\lambda^{q\mu} \\ \mathcal{A}_\lambda^{\mu qq} & \mathcal{A}_\lambda^{qq\mu} \end{bmatrix} \equiv -\lambda^\nu \partial_\mu \begin{bmatrix} \mathcal{R}_\lambda^{\nu q} & \mathcal{R}_\lambda^{q\nu} \\ \mathcal{R}_\lambda^{\nu qq} & \mathcal{R}_\lambda^{qq\nu} \end{bmatrix}. \tag{14}$$

The coefficient $L_{ww}$ does not admit a geometric representation. It is, however, subject to the geometric bound

$$L_{ww} = \tau \int_0^\tau dt\, \mathcal{G}_{\lambda_t}^{\mu\nu} \dot{\lambda}_t^\mu \dot{\lambda}_t^\nu \geqslant \mathcal{L}^2 \quad \text{with} \quad \mathcal{L} \equiv \oint_\gamma \sqrt{\mathcal{G}_\lambda^{\mu\nu} d\lambda^\mu d\lambda^\nu} \tag{15}$$

being the thermodynamic length of the path $\gamma$. This notion is motivated by the fact that, due to the second law, the coefficients $\mathcal{G}_\lambda^{\mu\nu} \equiv (\mathcal{R}_\lambda^{\mu\nu} + \mathcal{R}_\lambda^{\nu\mu})/2$ form a positive-semidefinite matrix and can therefore be interpreted as a pseudo-Riemannian metric in the space of control parameters. The bound (15) can be derived by minimizing $L_{ww}$ with respect to the parametrization of the path $\gamma$. A similar optimization is used in [46]. Here we make $L_{ww}$ a functional of a yet undetermined, monotonically increasing speed function $\phi_t$ and its derivative $\dot{\phi}_t$ through substitution $\lambda_t^\mu \to \lambda_{\phi_t}^\mu$. Solving the Euler-Lagrange equations for this functional with respect to the boundary conditions $\phi_0 = 0$ and $\phi_\tau = \tau$ yields the optimal parametrization $\phi_t$, for which Eq. (15) becomes an equality. This optimal speed function is implicitly given by

$$t = \frac{\tau}{\mathcal{L}} \int_0^{\phi_t} ds\, \sqrt{\mathcal{G}_{\lambda_s}^{\mu\nu} \dot{\lambda}_s^\mu \dot{\lambda}_s^\nu}. \tag{16}$$

Equations (13) and (15) show that the figure of merit $Z$ is subject to the bound $Z \leqslant \mathcal{Z} \equiv L_{qw}^3/4(L_{wq}^q + L_{qw}^q)\mathcal{L}^2$, where $\mathcal{Z}$ depends only on geometric quantities. Thus, Eqs. (9) and (10) imply the geometric tradeoff relations

$$J_q \leqslant \mathcal{Z}(\varepsilon_C - \varepsilon)^2/\varepsilon_C^2 \quad \text{and} \quad P \leqslant \mathcal{Z}(\eta_C - \eta)^2/\eta_C, \tag{17}$$

for adiabatic refrigerators and heat engines. These bounds, which are our second main result, hold for any thermodynamically consistent dynamics that admits a well-defined adiabatic-response regime. Moreover, they are asymptotically saturated in the limit $A_w \to 0$ if the optimal parametrization $\phi_t$ is chosen for the control path $\gamma$ and the thermal gradient scales with the driving frequency as $A_q = \mp\sqrt{\hat{z}A_w}$ with $\hat{z} \equiv \mathcal{L}^2/(L_{wq}^q + L_{qw}^q)$.

*Example: Two-stroke refrigerator.* Two-stroke cycles provide a general mechanism to fully suppress heat leaks, i.e., $J_q^{qs} = 0$. Under this protocol, the working system is decoupled from the environment for the first part $\tau_1 < \tau$ of the cycle and decoupled from the reservoir during the second part $\tau - \tau_1$. As a result, no persistent heat current between reservoir and environment emerges and $j_t$ and $J_q$ vanish for $A_w \to 0$. The coefficients (13) then depend solely on the equilibrium properties of the working system and the geometric figure of merit becomes

$$\mathcal{Z} = \frac{(\mathcal{S}_{\lambda_1} - \mathcal{S}_{\lambda_0})^3}{2\beta_e^3(\mathcal{C}_{\lambda_1} + \mathcal{C}_{\lambda_0})\mathcal{L}^2}, \tag{18}$$

where $\boldsymbol{\lambda}_1 \equiv \boldsymbol{\lambda}_{\tau_1}$ and $\mathcal{S}_\lambda$ and $\mathcal{C}_\lambda$ denote the equilibrium entropy and the heat capacity of the working system at fixed control parameters and inverse temperature $\beta_e$ [67]. Hence, the only quantity that still depends on the dynamics of the system is the thermodynamic length $\mathcal{L}$.

To illustrate the two-stroke mechanism, we consider a quantum refrigerator that consists of a qubit with Hamiltonian
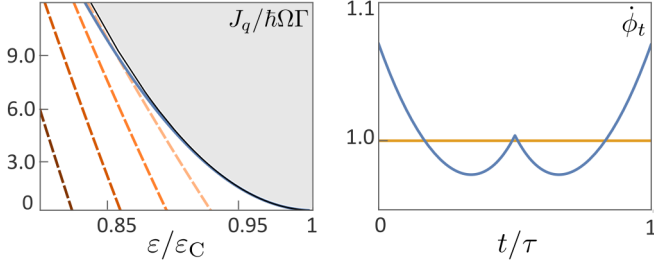
FIG. 1. Qubit refrigerator. The first plot shows the cooling power in units of $10^{-4}\hbar\Omega\Gamma$ as a function of the normalized COP, where $\tau$ is varied from $10^{-6}/\Gamma$ to $1/\Gamma$. Along the dashed lines, for which $1/\beta_r = 0.89,\ldots,0.95\hbar\Omega$ from left to right, the cooling power goes to zero at $\varepsilon/\varepsilon_C < 1$ in the limit $A_w \to 0$. The solid blue line, for which we set $A_q = -\sqrt{\hat{z}A_w}$, almost saturates the geometric bound (17), shown by the boundary of the gray-shaded region. For all plots, we have set $1/\beta_e = \hbar\Omega$ and chosen the optimal parametrization of the control path $\phi_t$, whose derivative is shown in the second plot.

$H_\lambda = \hbar\Omega\lambda\sigma_z/2$, where $\Omega$ sets the energy scale [24,69,70]. The state $\rho_t$ of the system evolves according to the adiabatic Lindblad equation [71]

$$\partial_t \rho_t = -\frac{i}{\hbar}[H_{\lambda_t}, \rho_t] + \mathsf{D}^r_{\lambda_t}\rho_t + \mathsf{D}^e_{\lambda_t}\rho_t \quad (19)$$

with $\mathsf{D}^x_\lambda \cdots \equiv \Gamma\kappa^x_t \sum_{\alpha=\pm} n^\alpha_{\lambda,\beta_x}([\sigma_\alpha \cdots, \sigma^\dagger_\alpha] + [\sigma_\alpha, \cdots \sigma^\dagger_\alpha])$ being dissipation superoperators that describe the influence of the reservoir and the environment (x = r, e). Here, $\sigma_z$ and $\sigma_\pm$ are the usual Pauli matrices, the rate $\Gamma > 0$ sets the relaxation timescale of the system, and $n^+_{\lambda,\beta_x} \equiv 1/(e^{\beta_x\hbar\Omega\lambda} - 1)$ and $n^-_{\lambda,\beta_x} \equiv n^+_{\lambda,\beta_x} + 1$ are thermal factors. For the control parameters $\lambda^1 \equiv \lambda$ and $\lambda^2 \equiv \kappa^r \equiv 1 - \kappa^e$, we choose the following protocols. During the first stroke, the system couples to the reservoir, i.e., $\kappa^r_t = 1$, and the level spacing $\lambda_t$ decreases linearly from 2 to 1; in the second stroke, the system couples to the environment, i.e., $\kappa^r_t = 0$, and $\lambda_t$ increases linearly from 1 to 2. For general adiabatic Lindblad dynamics, the generalized forces and the heat current are given by

$$f^\mu_t = -\mathrm{tr}\big[\rho^\tau_t \partial_\mu H_{\lambda_t}\big] \quad \text{and} \quad j_t = \mathrm{tr}\big[(\mathsf{D}^r_{\lambda_t}\rho^\tau_t)H_{\lambda_t}\big], \quad (20)$$

where $\rho^\tau_t$ is the periodic state of the system. These quantities can now be calculated perturbatively in the driving rates and the thermal gradient, which yields the thermodynamic length (15) and the figure of merit (18) for the qubit refrigerator [67]. To compare the performance of this device with the first tradeoff relation (17), we calculate its COP and cooling power by solving the master equation (19) numerically. Figure 1 shows that, in the quasistatic limit, $\varepsilon$ remains indeed strictly smaller than $\varepsilon_C$ for any fixed $A_q < 0$, while it approaches $\varepsilon_C$ if $A_q$ is optimized with respect to the cycle time; the bound (17) is asymptotically saturated if the optimal parametrization (16) is chosen for the control path.

This result shows that the sudden changes of the coupling parameters $\kappa^r$ and $\kappa^e$ are consistent with the adiabatic-response assumption. This conclusion holds in general for the weak-coupling regime, where the internal energy and the equilibrium state of the system do not depend on its interaction with the baths. Under this condition, the coupling
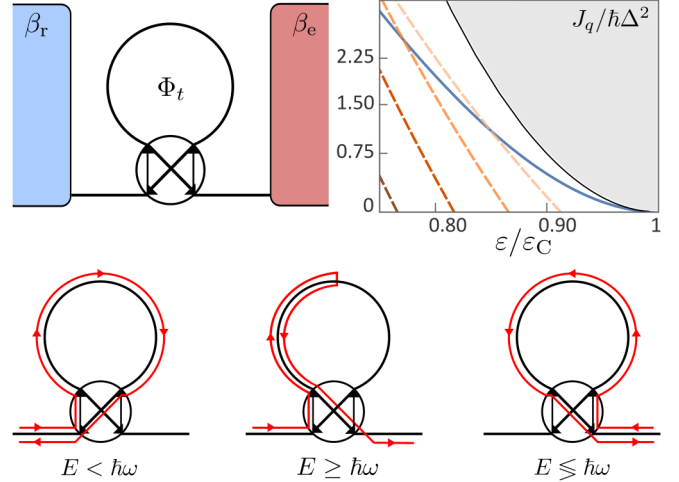


FIG. 2. Aharonov-Bohm refrigerator. A four-way beam splitter connects a mesoscopic ring and two ideal leads supporting a single transport channel. The left and right leads are coupled to the cold reservoir and the environment, respectively. The linearly increasing magnetic flux $\Phi_t$ induces a constant electromagnetic force around the ring, which decelerates incoming carriers from the reservoir; carriers with energy $E \geqslant \hbar\omega$ pass through the ring and return to the reservoir; carriers with $E < \hbar\omega$ are reflected on the ring and transmitted to the environment. Incoming carriers from the environment are accelerated and return to the environment regardless of their energy. For $\omega \to 0$, no carriers are transmitted; hence, the quasistatic heat flux vanishes. The plot shows the cooling power of the device in units of $10^{-4}\hbar\Delta^2$ as a function of its normalized COP, where $\omega$ is varied from $10^{-7}\Delta$ to $10^{-2}\Delta$. Here, $2\pi/\Delta = 4\pi m l^2/\hbar$ is the typical dwell time, $m$ denotes the carrier mass, and $l$ is the circumference of the ring. The dashed lines correspond to $1/\beta_r = 0.90,\ldots,0.96\hbar\Delta$ from left to right. The blue line is obtained for $A_q = -\sqrt{\hat{z}A_w}$, and the gray area indicates the bound (17). For all plots, we have set $1/\beta_e = \hbar\Delta$ and $\mu = 1.05\hbar\Delta$ and used the optimal parametrization $\phi_t = t$.

parameters do not give rise to generalized forces and their time derivatives do not appear in the expansion (12a); see [67] for details. As a result, the coupling parameters do not enter the diagonal kinetic coefficient (15) or the thermodynamic length. They rather affect only the off-diagonal coefficients (13), which, being geometric quantities, do not depend on the driving rates. The expansions (6) of the generalized fluxes are thus well-defined for the two-stroke protocol.

*Example: Aharonov-Bohm refrigerator.* To show that the tradeoff relations (17) are applicable also outside the two-stroke scheme, we now consider a mesoscopic refrigerator based on coherent transport. This example will show that heat leaks can be fully suppressed, even if both the environment and the reservoir couple to the system simultaneously. The system consists of a four-way beam-splitter and a mesoscopic ring subject to the time-dependent magnetic flux $\Phi_t$; see Fig. 2 [72]. Its two control parameters can be identified with the real and the imaginary parts of the Aharonov-Bohm phase, which are picked by a particle when passing through the ring, i.e., $e^{iq\Phi/\hbar c} \equiv \lambda^1 + i\lambda^2$, where $c$ is the speed of light and $q$ is the carrier charge. A linearly increasing flux, $\Phi_t \equiv \hbar c\omega t/q$, thus leads to the driving protocols $\lambda^1_t = \cos[\omega t]$ and $\lambda^2_t = \sin[\omega t]$, where $\omega = 2\pi/\tau$.

For coherent transport and effectively noninteracting carriers, the generalized forces and the heat current admit the general expressions [41,73,74]

$$f_t^\mu = -\int_0^\infty dE \sum_{x=r,e} \langle \psi_{E,t}^x | \partial_\mu H_{\lambda_t} | \psi_{E,t}^x \rangle g_E^x, \quad (21a)$$

$$j_t = \int_0^\infty dE \sum_{x=r,e} \langle \psi_{E,t}^x | J_{\lambda_t} | \psi_{E,t}^x \rangle g_E^x. \quad (21b)$$

Here, $H_\lambda$ and $J_\lambda$ are the single-carrier Hamiltonian and heat current operator, and $|\psi_{E,t}^x\rangle$ is the Floquet scattering state that describes a carrier with energy $E$, which enters the system either from the reservoir or the environment [74,75]; $g_E^x \equiv 1/[1 + e^{\beta_x(E-\mu)}]$ is the Fermi function with chemical potential $\mu$.

If the typical dwell time of carriers inside the system is short compared to $\tau$, the Floquet-scattering states can be calculated perturbatively [41], which yields the figure of merit $\mathcal{Z}$ for the Aharonov-Bohm refrigerator [67]. Since no carriers are transmitted for $\omega = 0$, the quasistatic heat flux vanishes and the first tradeoff relation (17) applies. Figure 2 shows how the cooling power and the COP of the Aharonov-Bohm refrigerator, which can be calculated exactly [67], compare to this bound in the slow-driving regime. As for the qubit-refrigerator, we find that $\varepsilon$ does not reach $\varepsilon_C$ for any fixed $A_q < 0$, while the tradeoff relation (17) is asymptotically saturated in the quasistatic limit if $A_q$ is optimized with respect to $A_w$.

*Concluding remarks.* Our findings for the Aharonov-Bohm refrigerator further underline the universality of our main insights. First, generic adiabatic thermal machines cannot approach their Carnot limit when working between two baths with a finite-temperature difference. Second, close to this limit, the performance of such devices is not captured by standard adiabatic-response theory, which treats both temperature gradient and driving rates as first-order perturbations. Instead,

second-order terms describing corrections to the finite-rate heat current and the nonisothermal work play an essential role. Taking these corrections into account leads to the geometric tradeoff relations (17), which imply that power decays quadratically rather than linearly at the Carnot bound. These results follow only from system-independent arguments and the Onsager symmetry (4).

For comparison, earlier bounds on the power of cyclic microscopic heat engines, which have been derived from Markov-jump, Fokker-Planck, or Lindblad dynamics, take the generic form $P \leqslant \xi \eta(\eta_C - \eta)$, where $\xi$ is a system-dependent figure of merit. These bounds hold arbitrarily far from equilibrium and require that the power output of the device vanishes at least linearly as its efficiency approaches the Carnot value. Our quadratic tradeoff relation (10) and its geometric counterpart (17), which have been derived from adiabatic-response theory, provide improvements of these earlier bounds for situations where a heat engine operating between two reservoirs with fixed temperatures approaches Carnot efficiency via the slow-driving limit. However, outside this setting, it is generally possible to devise engine cycles whose power decays linearly towards the Carnot bound; see, for instance, [14,25]. Whether there exist general bounds on the power of microscopic thermal machines that hold far from equilibrium and reduce to our geometric tradeoff relations (17) in the adiabatic-response regime remains as an important question for future research. Furthermore, even within the adiabatic-response framework, it would be interesting to explore how breaking the Onsager symmetry (4) alters the performance of thermal machines close to the Carnot limit.

[1] H. B. Callen, *Thermodynamics and an Introduction to Thermostatistics*, 2nd ed. (Wiley, New York, 1985).

[2] G. Benenti, K. Saito, and G. Casati, Thermodynamic Bounds on Efficiency for Systems with Broken Time-Reversal Symmetry, Phys. Rev. Lett. **106**, 230602 (2011).

[3] K. Brandner, K. Saito, and U. Seifert, Strong Bounds on Onsager Coefficients and Efficiency for Three-Terminal Thermoelectric Transport in a Magnetic Field, Phys. Rev. Lett. **110**, 070603 (2013).

[4] A. E. Allahverdyan, K. V. Hovhannisyan, A. V. Melkikh, and S. G. Gevorkian, Carnot Cycle at Finite Power: Attainability of Maximal Efficiency, Phys. Rev. Lett. **111**, 050601 (2013).

[5] V. Holubec and A. Ryabov, Maximum efficiency of low-dissipation heat engines at arbitrary power, J. Stat. Mech. (2016) 073204.

[6] M. Campisi and R. Fazio, The power of a critical heat engine, Nat. Commun. **7**, 11895 (2016).

[7] M. Polettini and M. Esposito, Carnot efficiency at divergent power output, Europhys. Lett. **118**, 40003 (2017).

[8] S. L. Lee and H. Park, Carnot efficiency is reachable in an irreversible process, Sci. Rep. **7**, 10725 (2017).

[9] V. Holubec and A. Ryabov, Diverging, but negligible power at Carnot efficiency: Theory and experiment, Phys. Rev. E **96**, 062107 (2017).

[10] V. Holubec and A. Ryabov, Cycling Tames Power Fluctuations near Optimum Efficiency, Phys. Rev. Lett. **121**, 120601 (2018).

[11] T. Koyuk, U. Seifert, and P. Pietzonka, A generalization of the thermodynamic uncertainty relation to periodically driven systems, J. Phys. A **52**, 02LT02 (2019).

[12] K. Miura, Y. Izumida, and K. Okuda, Compatibility of Carnot efficiency with finite power in an underdamped Brownian Carnot cycle in small temperature-difference regime, Phys. Rev. E **103**, 042125 (2021).

[13] K. Brandner and U. Seifert, Bound on thermoelectric power in a magnetic field within linear response, Phys. Rev. E **91**, 012121 (2015).

[14] K. Brandner, K. Saito, and U. Seifert, Thermodynamics of Micro- and Nano-Systems Driven by Periodic Temperature Variations, Phys. Rev. X **5**, 031019 (2015).

[15] K. Proesmans and C. Van den Broeck, Onsager Coefficients in Periodically Driven Systems, Phys. Rev. Lett. **115**, 090601 (2015).

[16] K. Proesmans, B. Cleuren, and C. Van den Broeck, Power-Efficiency-Dissipation Relations in Linear Thermodynamics, Phys. Rev. Lett. **116**, 220601 (2016).

[17] K. Yamamoto, O. Entin-Wohlman, A. Aharony, and N. Hatano, Efficiency bounds on thermoelectric transport in magnetic fields: The role of inelastic processes, Phys. Rev. B **94**, 121402(R) (2016).

[18] K. Brandner and U. Seifert, Periodic thermodynamics of open quantum systems, Phys. Rev. E **93**, 062134 (2016).

[19] N. Shiraishi, K. Saito, and H. Tasaki, Universal Trade-Off Relation between Power and Efficiency for Heat Engines, Phys. Rev. Lett. **117**, 190601 (2016).

[20] P. Pietzonka and U. Seifert, Universal Trade-Off between Power, Efficiency, and Constancy in Steady-State Heat Engines, Phys. Rev. Lett. **120**, 190602 (2018).

[21] T. Koyuk and U. Seifert, Operationally Accessible Bounds on Fluctuations and Entropy Production in Periodically Driven Systems, Phys. Rev. Lett. **122**, 230601 (2019).

[22] T. Kamijima, S. Otsubo, Y. Ashida, and T. Sagawa, Higher-order efficiency bound and its application to nonlinear nanothermoelectrics, Phys. Rev. E **104**, 044115 (2021).

[23] N. Shiraishi and K. Saito, Fundamental relation between entropy production and heat current, J. Stat. Phys. **174**, 433 (2019).

[24] P. A. Erdman, V. Cavina, R. Fazio, F. Taddei, and V. Giovannetti, Maximum power and corresponding efficiency for two-level heat engines and refrigerators: optimality of fast cycles, New J. Phys. **21**, 103049 (2019).

[25] P. Menczel, C. Flindt, and K. Brandner, Quantum jump approach to microscopic heat engines, Phys. Rev. Research **2**, 033449 (2020).

[26] R. S. Whitney, Most Efficient Quantum Thermoelectric at Finite Power Output, Phys. Rev. Lett. **112**, 130601 (2014).

[27] R. S. Whitney, Finding the quantum thermoelectric with maximal efficiency and minimal entropy production at given power output, Phys. Rev. B **91**, 115425 (2015).

[28] E. Potanina, C. Flindt, M. Moskalets, and K. Brandner, Thermodynamic Bounds on Coherent Transport in Periodically Driven Conductors, Phys. Rev. X **11**, 021013 (2021).

[29] K. Miura, Y. Izumida, and K. Okuda, Achieving Carnot efficiency in a finite-power Brownian Carnot cycle with arbitrary temperature difference, Phys. Rev. E **105**, 034102 (2022).

[30] F. Weinhold, Metric geometry of equilibrium thermodynamics, J. Chem. Phys. **63**, 2479 (1975).

[31] R. Gilmore, Length and curvature in the geometry of thermodynamics, Phys. Rev. A **30**, 1994 (1984).

[32] B. Andresen, R. S. Berry, R. Gilmore, E. Ihrig, and P. Salamon, Thermodynamic geometry and the metrics of Weinhold and Gilmore, Phys. Rev. A **37**, 845 (1988).

[33] G. Ruppeiner, Riemannian geometry in thermodynamic fluctuation theory, Rev. Mod. Phys. **67**, 605 (1995).

[34] G. E. Crooks, Measuring Thermodynamic Length, Phys. Rev. Lett. **99**, 100602 (2007).

[35] D. A. Sivak and G. E. Crooks, Thermodynamic Metrics and Optimal Paths, Phys. Rev. Lett. **108**, 190602 (2012).

[36] P. R. Zulkowski, D. A. Sivak, G. E. Crooks, and M. R. DeWeese, Geometry of thermodynamic control, Phys. Rev. E **86**, 041148 (2012).

[37] B. B. Machta, Dissipation Bound for Thermodynamic Control, Phys. Rev. Lett. **115**, 260603 (2015).

[38] P. W. Brouwer, Scattering approach to parametric pumping, Phys. Rev. B **58**, R10135(R) (1998).

[39] M. Scandi and M. Perarnau-Llobet, Thermodynamic length in open quantum systems, Quantum **3**, 197 (2019).

[40] H. J. D. Miller, M. Scandi, J. Anders, and M. Perarnau-Llobet, Work Fluctuations in Slow Processes: Quantum Signatures and Optimal Control, Phys. Rev. Lett. **123**, 230603 (2019).

[41] M. Thomas, T. Karzig, S. V. Kusminskiy, G. Zaránd, and F. von Oppen, Scattering theory of adiabatic reaction forces due to out-of-equilibrium quantum environments, Phys. Rev. B **86**, 195419 (2012).

[42] M. F. Ludovico, F. Battista, F. von Oppen, and L. Arrachea, Adiabatic response and quantum thermoelectrics for ac-driven quantum systems, Phys. Rev. B **93**, 075136 (2016).

[43] V. Cavina, A. Mari, and V. Giovannetti, Slow Dynamics and Thermodynamics of Open Quantum Systems, Phys. Rev. Lett. **119**, 050601 (2017).

[44] R. Bustos-Marún, G. Refael, and F. von Oppen, Adiabatic Quantum Motors, Phys. Rev. Lett. **111**, 060802 (2013).

[45] P. Abiuso and M. Perarnau-Llobet, Optimal Cycles for Low-Dissipation Heat Engines, Phys. Rev. Lett. **124**, 110606 (2020).

[46] K. Brandner and K. Saito, Thermodynamic Geometry of Microscopic Heat Engines, Phys. Rev. Lett. **124**, 040602 (2020).

[47] H. J. D. Miller and M. Mehboudi, Geometry of Work Fluctuations Versus Efficiency in Microscopic Thermal Machines, Phys. Rev. Lett. **125**, 260602 (2020).

[48] Y. Izumida, Hierarchical Onsager symmetries in adiabatically driven linear irreversible heat engines, Phys. Rev. E **103**, L050101 (2021).

[49] Y. Hino and H. Hayakawa, Geometrical formulation of adiabatic pumping as a heat engine, Phys. Rev. Research **3**, 013187 (2021).

[50] B. Bhandari and A. N. Jordan, Continuous measurement boosted adiabatic quantum thermal machines, arXiv:2112.03971.

[51] H. J. D. Miller, M. H. Mohammady, M. Perarnau-Llobet, and G. Guarnieri, Thermodynamic Uncertainty Relation in Slowly Driven Quantum Heat Engines, Phys. Rev. Lett. **126**, 210603 (2021).

[52] A. G. Frim and M. R. DeWeese, A geometric bound on the efficiency of irreversible thermodynamic cycles, arXiv:2112.10797.

[53] H. Hayakawa, V. M. M. Paasonen, and R. Yoshii, Geometrical quantum chemical engine, arXiv:2112.12370.

[54] J. Lu, Z. Wang, J. Peng, C. Wang, J.-H. Jiang, and J. Ren, Geometric thermodynamic uncertainty relation in a periodically driven thermoelectric heat engine, Phys. Rev. B **105**, 115428 (2022).

[55] J. Monsel, J. Schulenborg, T. Baquet, and J. Splettstoesser, Geometric energy transport and refrigeration with driven quantum dots, arXiv:2202.12221.

[56] B. Bhandari, P. T. Alonso, F. Taddei, F. von Oppen, R. Fazio, and L. Arrachea, Geometric properties of adiabatic quantum thermal machines, Phys. Rev. B **102**, 155407 (2020).

[57] N. Pancotti, M. Scandi, M. T. Mitchison, and M. Perarnau-Llobet, Speed-Ups to Isothermality: Enhanced Quantum Thermal Machines through Control of the System-Bath Coupling, Phys. Rev. X **10**, 031015 (2020).

[58] P. Abiuso, H. J. D. Miller, M. Perarnau-Llobet, and M. Scandi, Geometric optimisation of quantum thermodynamic processes, Entropy **22**, 1076 (2020).

[59] R. Xu, A numerical method to find the optimal thermodynamic cycle in microscopic heat engine, J. Stat. Phys. **184**, 29 (2021).

[60] P. Terrén Alonso, P. Abiuso, M. Perarnau-Llobet, and L. Arrachea, Geometric optimization of nonequilibrium adiabatic thermal machines and implementation in a qubit system, PRX Quantum **3**, 010326 (2022).

[61] V. Cavina, P. A. Erdman, P. Abiuso, L. Tolomeo, and V. Giovannetti, Maximum-power heat engines and refrigerators in the fast-driving regime, Phys. Rev. A **104**, 032226 (2021).

[62] G. Watanabe and Y. Minami, Finite-time thermodynamics of fluctuations in microscopic heat engines, Phys. Rev. Research **4**, L012008 (2022).

[63] P. A. Erdman and F. Noe, Identifying optimal cycles in quantum thermal machines with reinforcement-learning, npj Quantum Inf. **8**, 1 (2022).

[64] U. Seifert, Stochastic thermodynamics, fluctuation theorems and molecular machines, Rep. Prog. Phys. **75**, 126001 (2012).

[65] S. H. Lee, J. Um, and H. Park, Nonuniversality of heat-engine efficiency at maximum power, Phys. Rev. E **98**, 052137 (2018).

[66] To see that $Z, z \geqslant 0$, first notice that the refrigerator condition $J_q \geqslant 0$ requires that $L_{qw} \geqslant 0$, since $J_q = L_{qw} A_w$ in leading order in the affinities and $A_w \geqslant 0$. Second, observe that the rate of entropy production is given by $\sigma = L_{ww} A_w^2 + (L_{qw}^q + L_{wq}^q) A_w A_q^2$ at leading order. The second law $\sigma \geqslant 0$ thus requires $L_{qw}^q + L_{wq}^q \geqslant 0$.

[67] See Supplemental Material at http://link.aps.org/supplemental/10.1103/PhysRevE.105.L052102 for a derivation of the bound (10), general adiabatic-response coefficients for Lindblad dynamics and coherent transport, and details on the qubit and Aharonov-Bohm refrigerators.

[68] For heat engines, the symmetry $L_{wq} \simeq -L_{qw}$ leads to the analogous relation $\eta = (1 - L_{ww} A_w / L_{qw} A_q) \eta_C$.

[69] A. O. Niskanen, Y. Nakamura, and J. P. Pekola, Information entropic superconducting microcooler, Phys. Rev. B **76**, 174523 (2007).

[70] B. Karimi and J. P. Pekola, Otto refrigerator based on a superconducting qubit: Classical and quantum performance, Phys. Rev. B **94**, 184503 (2016).

[71] T. Albash, S. Boixo, D. A. Lidar, and P. Zanardi, Quantum adiabatic markovian master equations, New J. Phys. **14**, 123016 (2012).

[72] J. E. Avron, A. Elgart, G. M. Graf, and L. Sadun, Optimal Quantum Pumps, Phys. Rev. Lett. **87**, 236601 (2001).

[73] N. Bode, S. V. Kusminskiy, and F. Egger, and R. von Oppen, Current-induced forces in mesoscopic systems: A scattering-matrix approach, Beilstein J. Nanotechnol. **3**, 144 (2012).

[74] K. Brandner, Coherent transport in periodically driven mesoscopic conductors: From scattering amplitudes to quantum thermodynamics, Z. Naturforsch. A **75**, 483 (2020).

[75] M. Moskalets and M. Büttiker, Floquet scattering theory of quantum pumps, Phys. Rev. B **66**, 205320 (2002).